SCRS/2014/125 Collect. Vol. Sci. Pap. ICCAT, 71(6): 2944-2957 (2015)

NONLINEAR FORECASTING OF SEA SURFACE TEMPERATURE EFFECTS ON BLUEFIN TUNA RECRUITMENT

Harford[1], W. J, Karnauskas[2], M., Walter[2], J. Liu[3], H.

SUMMARY

Environment-recruitment relationships can be difficult to delineate with traditional statistical models. We use state-space reconstruction techniques, which are non-parametric and make no assumptions about functional relationships, to address the question of whether environmental influences on early life stages can be used to forecast subsequent recruitment. We find that sea surface temperature, which has been associated with larval growth and survival, can be used to improve one-year ahead forecasts of bluefin tuna recruitment. This result was found for areas surrounding the Balearic Archipelago (Mediterranean Stock), the Gulf of Mexico, and areas east of Chinese Taipei and within the Sea of Japan (North Pacific Stock). Our analysis does not negate the importance of stock-recruitment functions for fisheries management; rather, it identifies the possibility of using alternative tools for recruitment forecasting. In particular, state-space reconstruction is expected to be useful when recruitment is poorly estimated by traditional methods, including instances where cohorts have not yet entered the fishery.

RÉSUMÉ

Les relations environnement-recrutement peuvent être difficiles à déterminer au moyen de modèles statistiques traditionnels. Nous utilisons des techniques de reconstruction état-espace, qui ne sont pas paramétriques et n'émette pas de postulat au sujet des relations fonctionnelles, afin de traiter la question de savoir si les influences environnementales sur les premiers stades du cycle vital peuvent être utilisées pour prédire le recrutement ultérieur. Nous avons constaté que la température de surface de la mer, qui a été associée à la croissance larvaire et à la survie, peut servir à améliorer les prévisions un an à l'avance du recrutement du thon rouge. Ce résultat est apparu pour des zones avoisinant l'archipel des Baléares (stock méditerranéen), le golfe du Mexique et des zones à l'Est du Taipei chinois et à l'intérieur de la mer du Japon (stock du Pacifique Nord). Notre analyse ne conteste pas l'importance des fonctions stock-recrutement pour la gestion des pêcheries, mais elle identifie la possibilité d'avoir recours à d'autres outils pour prédire le recrutement. Plus particulièrement, la reconstruction état-espace devrait être utile lorsque le recrutement est mal estimé par les méthodes traditionnelles, y compris les cas où des cohortes ne sont pas encore entrées dans la pêcherie.

RESUMEN

Las relaciones medio ambiente-reclutamiento pueden ser difíciles de establecer con los modelos estadísticos tradicionales. Se usan técnicas de reconstrucción estado-espacio, que son no paramétricas y no hacen supuestos acerca de relaciones funcionales para solucionar la cuestión de si las influencias medioambientales en las primeras etapas de vida pueden usarse para prever el posterior reclutamiento. Se halló que la temperatura de la superficie del mar (SST), que se había asociado con el crecimiento de larvas y las tasas de supervivencia, puede utilizarse para mejorar las previsiones de futuro de un año del reclutamiento de atún rojo. Este resultado se halló en el archipiélago balear (stock del Mediterráneo), en el golfo de México, en zonas al este de Taipei Chino y dentro del mar de Japón (stock del Pacífico septentrional). Nuestro análisis no niega la importancia de las funciones stock-reclutamiento para la ordenación pesquera, en su lugar, identifica la posibilidad de utilizar herramientas alternativas para la previsión del reclutamiento. En particular, se prevé que la reconstrucción estado-espacio sea útil cuando se dispone de una estimación mediocre del reclutamiento mediante los métodos tradicionales, lo que incluye los casos en los que las cohortes no han entrado todavía en la pesquería.

KEYWORDS

Recruitment, Environmental effects, Surface temperature, Tuna fisheries

[1] Cooperative Institute for Marine and Atmospheric Studies, Rosenstiel School of Marine and Atmospheric Science, University of Miami, Miami, FL, USA, 33149; william.harford@noaa.gov

[2] NOAA National Marine Fisheries Service, Southeast Fisheries Science Center, Sustainable Fisheries Division, Miami, FL, USA, 33149.

[3] Marine Biology Department, Texas A&M University at Galveston, Galveston, TX, USA, 77553.

1. Introduction

Ways in which environmental conditions affect fish recruitment has previously received investigation in fisheries ecology (Myers *et al.* 1993, Alheit and Hagen 1997, Govoni 2005). Problematically though, correlations between environmental and biological variables can be difficult to delineate and can sometimes appear ephemeral in nature (Sugihara *et al.* 2012). Finding evidence of environmental drivers can be plagued by inconsistencies that can appear as positively correlated variables at some times and as uncorrelated or negatively correlated variables at other times (Myers 1998, Carscadden *et al.* 2000, Ravier and Fromentin 2004). One possible explanation for inconsistencies in environment-recruitment relationships is the use of traditional linear statistical methods in instances where biological systems are nonlinear (Hsieh *et al.* 2005, 2008, Glaser *et al.* 2013). Nonlinearity in biological systems can arise from non-additive interactions among forcing variables (Steele and Henderson 1984, Sugihara 1994, Dixon *et al.* 1999, Glaser *et al.* 2011). Where traditional linear modeling is insufficient to capture the complexity of nonlinear systems, a more robust approach is offered by state-space reconstruction (SSR; Deyle and Sugihara 2011, Deyle *et al.* 2013). Techniques for SSR offer the flexibility to delineate both linear and nonlinear dynamics (Sugihara *et al.* 2012, Deyle *et al.* 2013). This flexibility is possible because SSR techniques are non-parametric and make no assumptions about functional relationships. Instead, SSR relies on the structure of the data to identify interacting variables, thus enabling accommodation of a variety of behaviors (Glaser *et al.* 2011, Perretti *et al.* 2013).

Atlantic and Pacific bluefin tuna (*Thunnus thynnus*, Scombridae; *Thunnus orientalis*, Scombridae) undergo extensive migrations as adults, but spawn in narrowly defined geographic areas (Garcia *et al.* 2005, Block *et al.* 2005, Fromentin and Powers 2005, Satoh *et al.* 2008). Observational studies have examined spawning and larval distributions of bluefin tuna in relation to environmental conditions (McGowan and Richards 1989, Davis *et al.* 1990, Kitagawa *et al.* 2000, Tanaka *et al.* 2007, Satoh 2010, Alemany *et al.* 2010, Lindo-Atichati *et al.* 2012, Muhling *et al.* 2013), but few studies examine whether and how environmental conditions experienced during larval development are likely to translate into recruitment fluctuations. Here, SSR techniques were used to address the question of whether environmental conditions, occurring in relation to timing of spawning and early life stages, could be detected in subsequent recruitment fluctuations. We applied a multivariate extension of SSR to evaluate whether and how sea surface temperature is related to recruitment dynamics. We explored the reliability of near-term recruitment forecasts produced from SSR relative to a simple alternative forecasting technique. The analysis was regarded as a precursor to the potential use of nonlinear time series modeling to complement recruitment forecasting techniques currently used in stock assessment procedures.

2. Methods

2.1 State-space reconstruction

State-space reconstruction (SSR) considers the structure of a one-dimensional (univariate) time series as having been produced from underlying ecological processes. Takens (1981) theorem shows that a dynamical system can be reconstructed through time-delayed coordinate embedding. Time-delayed coordinate embedding involves transforming a univariate time series into a set of time-delayed vectors:

$$\mathbf{X}_t = \left[x_t, x_{t-\tau}, x_{t-2\tau}, \ldots, x_{t-(E-1)\tau} \right], \tag{1}$$

where x is a time series, t is time, τ is the time lag, and E is the embedding dimension. The embedding dimension is the number of time-delayed coordinates used in state-space reconstruction (Sugihara and May 1990, Glaser *et al.* 2013). Time-delayed vectors capture properties of the unknown state space attractor (Takens 1981, Sugihara and May 1990, Deyle and Sugihara 2011).

The univariate SSR approaches we applied were simplex projection and S-maps techniques developed by Sugihara and May (1990) and Sugihara (1994), respectively. The simplex projection model was used to identify the best embedding dimension for the time series (Sugihara and May 1990). Simplex projection is a nearest neighbor algorithm that uses the shape of the reconstructed attractor in E-dimensions to predict the trajectory of the time series from time t to time $t+1$. Simplex projection contains only one parameter, E, which is sequentially varied from 1 to 10. In model fitting, the coordinate vectors are divided into sets of library vectors and prediction vectors. To generate forecasts of the prediction vectors, Euclidean distances to all library vectors are calculated, and the $E+1$ nearest neighbors are used to generate an exponentially weighted prediction:

$$\hat{x}_T = \sum_{j=0}^{E} w_j x_T(j), \quad (2)$$

where weightings, w_j, for each neighbor *j*, are determined at time *t*, and applied to forecasts of the prediction vector, $\hat{x}_T$, at *T=t+1*. This means that library coordinate vectors that are similar to the prediction vector at time *t* and are also expected to have similar states at *t+1*. Because our recruitment time series tended to be short, out-of-sample forecast skill was tested using leave-one-out cross-validation (Sugihara *et al.* 1996, Glaser *et al.* 2011, 2013, Liu *et al.* 2014). Forecast skill was defined as the Pearson correlation coefficient (ρ) and mean absolute error (MAE) calculated from observed and forecasted values.

After identifying *E* that produced the highest forecast skill, sequentially weighted global linear maps (S-maps) were used to explore evidence on nonlinearity. S-maps examine evidence of nonlinearity by comparing the forecast skill obtained using equivalent linear or nonlinear models. Implementation details are described by Sugihara (1994), and summarily by Glaser *et al.* (2011), Liu *et al.* (2012), Sugihara *et al.* (2012), Glaser *et al.* (2013), and Deyle *et al.* (2013), and Liu *et al.* (2014). Briefly, forecasts at time *t+1* are made using all library vectors, rather than *E+1* nearest neighbors used in simplex projection, but where library vectors are still weighted according to according to Euclidean distance from the prediction vector. Forecasts produced by S-maps are tuned by adjusting a nonlinearity parameter, θ, within the continuous range of 0 to 10. The nonlinearity parameter controls how heavily library vectors that are nearest to the prediction vector are weighed relative to distant library vectors:

$$w(d) = \exp\left(-\theta d / \overline{d}\right), \quad (3)$$

where *d* is Euclidean distance and $\overline{d}$ is the minimum distance from all library vectors. When $\theta = 0$ all library vectors are given equal weight and S-maps give linear forecasts. Higher θ values give greater weight to library vectors that are in close proximity to the prediction vector. Since specifying the model as linear ($\theta = 0$) or nonlinear ($\theta > 0$) depends on only one parameter, it is convenient to test whether nonlinear forecast skill is significantly improved over linear forecast skill. We calculated the decrease in forecast error ($\Delta\text{MAE} = \text{MAE}_{\theta=0} - \text{MAE}_{\theta=\text{best}}$) as a measure of nonlinearity (Hsieh and Ohman 2006). Permutation testing was implemented by first calculating the test statistic, ΔMAE, then shuffling the time series before carrying out the S-map procedure. Null ΔMAE was then calculated from the S-map procedure applied to the shuffled time series. This process was repeated 1000 times and significant improvement in forecasting skill using a nonlinear model was determined using a cutoff p-value of 0.05 (Hsieh and Ohman 2006).

Deyle and Sugihara (2011) generalized Takens' (1981) approach to situations when multiple time series from the same system are analyzed together. Multivariate SSR examines whether variable *x* and an auxiliary variable *y* are interacting parts of the same system. Multivariate embedding consists of including *y* in the construction of time delayed coordinates (e.g., $\left[x_t, x_{t-\tau}, x_{t-2\tau}, \ldots, x_{t-(E-1)\tau}, y_t \right]$). Multivariate SSRs were compared to the univariate SSR to determine whether multivariate embedding led to significant improvement in forecast skill. We first calculated the improvement in forecast skill ($\Delta\rho$) between univariate and multivariate coordinate embeddings. We then tested whether improvement in fit was different from improvement expected by chance alone. Permutation testing was implemented by shuffling the forcing variable, *y*, and calculating the null forecast improvement. These steps were repeated 1000 times, the fraction of instances in which null forecast improvement exceeded the predicted forecast skill provided the probability that forecast improvement occurred by chance alone. Significant improvement in forecasting skill was considered to be evident when the probability of forecast improvement occurring by chance alone was <0.10.

2.2 Forecast performance

We evaluated whether recruitment forecasts made by multivariate SSR were more reliable than other simple predictive approaches. Performance was measured using standardized root mean square error (SRMSE), which is the RMSE divided by the standard deviation of the dataset used in prediction. Values of SRMSE greater than 1 indicate that forecasting models are less accurate than using the mean of the dataset for prediction (Perretti *et al.* 2013). For each recruitment time series, we compared the multivariate SSR to univariate SSR and the naïve forecasting method, which uses recruitment in year *t* as a predictor at time *t+1*.

2.3 Time series

Time series of Atlantic bluefin tuna recruits and spawning stock biomass (SSB) were available for the period of 1950-2013 for the eastern Atlantic stock and 1970-2013 for the western Atlantic stock (Anon., 2013). Estimates of recruitment in numbers of age-1 individuals were obtained from virtual population analysis (VPA). VPA-based estimates were used because VPA does not impose a stock-recruitment function on recruitment estimates. For our analysis, we excluded the years 2004-2013 from the eastern stock and 2011-2013 from the western stock because these most recent estimates could be prone to estimation inaccuracies, including retrospective bias (Anon., 2013). Time series of Pacific bluefin tuna recruitment of age-0 individuals was obtained for the period of 1952-2012 (Anon., 2015). Our analysis included recruitment between 1953-2008 (Anonymous 2015). For each of the stocks, we also obtained spawning stock biomass time series to explore this variable as a driver of recruitment dynamics.

Prior to model fitting, recruitment time series were processed by taking first differences ($\Delta x = x_t - x_{t-1}$) and normalizing (i.e. mean = 0, standard deviation = 1).

2.4 Sea surface temperature

Sea surface temperatures (SST) were obtained from the International Comprehensive Ocean-Atmosphere Data Set (ICOADS; National Climatic Data Center/NESDIS/NOAA/U.S. n.d.). Non-interpolated monthly mean temperatures were obtained at 2-degree spatial resolution (National Climatic Data Center/NESDIS/NOAA/U.S. n.d.). SST was extracted for areas of known bluefin tuna spawning and where larvae are commonly collected (Figs. 1A, 2A, 3A). In the Mediterranean Sea, two rectangles were specified that focused on waters surrounding the Belearic Archipelago (Garcia *et al.* 2005, Alemany *et al.* 2010). The largest rectangle covered the area between 38º and 40º North and between 1º and 5º East, which was consistent with the extent of TUNIBAL surveys conducted by the *Instituto Español de Oceanografía* (**Figure 1A**; Garcia *et al.* 2005, Alemany *et al.* 2010). A smaller rectangular area was also considered between 37.5º and 39.5º North and between 3º and 5º East, which covered the area south of the archipelago where the high larval densities has been reported (Alemany *et al.* 2010). In the Gulf of Mexico, three regions were defined: the immediate region of influence (ROI) of the Loop Current in the spring season (between 25º and 27º North and between 86º and 88º West), a region to the west of the loop current that is associated with spawning and larval habitat (between 25º and 28º North and between 88º and 95º West), and a region north of the Loop Current (between 27º and 29º North and between 84º and 98º West) (**Figure 2A**; Teo *et al.* 2007, Lindo-Atichati *et al.* 2012, Muhling *et al.* 2013). In the North Pacific, we considered three regions associated with spawning: an area east of Chinese Taipei (between 22.5º and 24.5º North and between 123.5º and 125.5º East), a larger region surrounding the RyuKyu Islands (between 22º and 26º North and between 124º and 130º East), and the eastern Sea of Japan (between 36º and 38º North and between 132º and 136º East). We also considered a coastal area south of Japan within the area of 32 º and 35º North and between 132 º and 141º East (Kitagawa *et al.* 2010).

3. Results

3.1 Atlantic bluefin tuna

Univariate SSR of eastern Atlantic recruitment (no environmental forcing used in forecasting), suggested that nonlinear forecast skill (ΔMAE) was not significantly improved over a linear S-map model (*p-value* = 0.279). When introducing SSB and SST into the SSR models, SSB and a SSTs in summer and autumn months tended to improve forecast skill in term of increasing ρ relative to equivalent univariate SSRs (**Table 1**). A multivariate forecast that included both SSB and September SST was constructed as an exploration of utilizing both biological and environmental data in recruitment forecasting ($\rho = 0.782$; **Figure 1**).

A nonlinear signature in forecast skill was detected in univariate forecasts of western Atlantic recruitment (ΔMAE , *p-value* = 0.001). Multivariate modeling revealed significant improvement in forecast skill when SSB was included state-space reconstruction (**Table 2**). When SSTs were considered in multivariate SSR, spring SSTs outside of the Loop Current ROI significantly improved forecast skill. In the area west of the Loop Current ROI, April SST improved recruitment forecasts, while in the area north of the Loop Current ROI, May SST similarly improved recruitment forecasts (**Table 2**). Including biological and environmental data in recruitment forecasting was explored by producing a multivariate forecast that included both SSB and April SST west of the Loop Current ($\rho = 0.455$; **Figure 2**).

3.2 North Pacific bluefin tuna

Univariate SSR of Pacific bluefin tuna recruitment indicated a nonlinear signature in forecast skill ($\Delta\mathrm{MAE}$, *p-value* = 0.003). When SST was included in the multivariate SSR, significant improvement in forecast skill was obtained when using the months following spawning in the Sea of Japan and near Chinese Taipei and the Ryukyu Islands (**Table 3**). Also evident was the potential effect of SST in the area south of Japan. SSTs within this area were not strongly correlated with SSTs within the spawning area to the southwest, thus it possible both areas independently influence recruitment. There was however, a strong positive correlation between the larger and smaller bounding boxes of the Ryukyu Island spawning area, suggesting a regional SST pattern was reflected in both datasets. In exploring SSRs that contained more than one auxiliary variable *y*, it was found that combinations of SST drivers, without inclusion of SSB, led to the highest forecast skill. As an example, August SSTs in the two spawning regions (Ryukyu Islands and Sea of Japan) produced forecast skill of $\rho = 0.340$ (**Figure 3**).

3.3 Forecast performance

Multivariate SSR provided more reliable one year-ahead forecasts of recruitment than univariate SSR or the naïve method. All SST and SSB variables reported in **Tables 1** through **3** produced improved forecast skill (ρ) relative to univariate forecasts. Likewise, multivariate SSR had lower SRMSE than univariate SSR, and in all cases, multivariate SSR models had lower SRMSE than the naïve forecast method. This result suggests that signals from SST and SSB improved overall forecast performance. However, when SRMSE estimates were compared to unity, not all multivariate SSRs produced appreciably better forecasts than would be expected by using the mean as a predictor (**Figure 4**). Taken together, forecast performance suggests that while recruitment fluctuations are to varying degrees correlated with SST, and thus SST can be used to improve forecasts, model improvements are still desirable. For each of the combined multivariate SSR forecasting models illustrated in **Figures 1b, 2b, & 3b**, forecast performance was contrasted against univariate and naïve modeling methods (**Figure 4**). Multivariate SSR performed particularly well in forecasting recruitment for the eastern Atlantic stock, with SRMSE values well below 1; however, performance was poorer for the western Atlantic and Pacific stocks (**Figure 4**).

4. Discussion

SSR techniques have been demonstratively useful for short-term forecasting of biological systems (Perretti *et al.* 2013, Glaser *et al.* 2013, Ward *et al.* 2014). Here, we found that nonlinear models that included sea surface temperatures (SST) could improve forecasts of bluefin tuna recruitment. Notably, significant improvements in out-of-sample forecasting were found only for SST variables in months that generally corresponded with the timing of bluefin tuna spawning. SST has previously been associated with larval development, thus, it is perhaps not surprising that SST in the months immediately following spawning appear to influence subsequent recruitment fluctuations. The eastern Atlantic stock spawns most commonly during June and July in the waters of the western Mediterranean Sea in proximity to the Balearic Archipelago and to Sicily (Garcia *et al.* 2005, Alemany *et al.* 2010, Muhling *et al.* 2013). Our analysis suggested that SSTs in September, 60-90 days post spawning, improved recruitment forecasts in the following year. The western Atlantic stock spawns in the Gulf of Mexico during April, May, and June (Block *et al.* 2005, Teo *et al.* 2007, Teo and Block 2010). During the months associated with spawning, adult bluefin tuna may avoid the Loop Current, which flows north from the Caribbean Sea, enters the Gulf of Mexico and loops eastward, eventually entering the Florida Straits (Lindo-Atichati *et al.* 2012). Accordingly, we found that forecasts were improved when April and May SSTs from areas sounding the Loop Current's region of influence were included in recruitment forecasts. North Pacific bluefin tuna spawn in proximity to the Ryukyu Islands and Chinese Taipei from April to June and in the Sea of Japan in August (Satoh 2010 and references therein). Similar to the findings for the Mediterranean Sea, SSTs approximately 2 to 4 months post spawning improved recruitment forecasts. Following hatching, and perhaps after a period of retention in anticyclonic eddies associated with Ryukyuan Islands, the Kuroshio Current appears to transport larvae to cooler coastal nursery grounds south of Japan (Kitagawa *et al.* 2006, 2010, Kimura *et al.* 2010). Larval growth and survival are widely cited as critical aspects of bluefin tuna biology, and particularly in relation to temperature (Matsuura *et al.* 1997, Masuda *et al.* 2002, Tanaka *et al.* 2006, Reglero *et al.* 2011).

From a fisheries management perspective, it was also intriguing that multivariate SSR provided better forecasts than simpler naïve forecasting methods. While more direct comparison of forecast skill with stock-recruitment functions is necessary, our analysis demonstrates an additional, but distinctly different tool for recruitment forecasting. Our analysis does not negate the importance of stock-recruitment functions for fisheries management; rather, multivariate SSR can be potentially useful to stock assessment by providing recruitment forecasts for cohorts that have not become fully vulnerable to fishing, and thus are not prevalent in catch-at-age matrices. Near-term forecasting of recruitment in future years is also possible, and could be useful for supporting model-based projections used in evaluating total catch regulations. Finally, our analyses demonstrated an initial step in moving from identification of environmental correlates to the use of environmental drivers in forward-forecasting of recruitment fluctuations.

References

Alemany, F., L. Quintanilla, P. Velez-Belchí, A. García, D. Cortés, J. M. Rodríguez, M. L. Fernández de Puelles, C. González-Pola, and J. L. López-Jurado. 2010. Characterization of the spawning habitat of Atlantic bluefin tuna and related species in the Balearic Sea (western Mediterranean). Progress in Oceanography 86:21-38.

Alheit, J., and E. Hagen. 1997. Long-term climate forcing of European herring and sardine populations. Fisheries Oceanography 6:130-139.

Anon., 2013. Report of the 2012 Atlantic bluefin tuna stock assessment session. September 22 to 27, 2014, Madrid, Spain. Collect. Vol. Sci. Pap. ICCAT, 69(1): 1-198.

Anon., 2015. Stock assessment of bluefin tuna in the Pacific Ocean in 2014. Report of the Pacific bluefin tuna working group. International Scientific Committee for Tuna and Tuna-like Species in the North Pacific Ocean. Collect. Vol. Sci. Pap. ICCAT, 71. *In this Volume.*

Block, B. A., S. L. H. Teo, A. Walli, A. Boustany, M. J. W. Stokesbury, C. J. Farwell, K. C. Weng, H. Dewar, and T. D. Williams. 2005. Electronic tagging and population structure of Atlantic bluefin tuna. Nature 434:1121-1127.

Carscadden, J. E., K. T. Frank, and W. C. Leggett. 2000. Evaluation of an environment–recruitment model for capelin (*Mallotus villosus*). ICES Journal of Marine Science: Journal du Conseil 57:412-418.

Davis, T. L. O., G. P. Jenkins, and J. W. Young. 1990. Diel patterns of vertical distribution in larvae of southern bluefin *Thunnus maccoyii*, and other tuna in the East Indian Ocean. Mar. Ecol. Prog. Ser 59:63-74.

Deyle, E. R., M. Fogarty, C. -h. Hsieh, L. Kaufman, A. D. MacCall, S. B. Munch, C. T. Perretti, H. Ye, and G. Sugihara. 2013. Predicting climate effects on Pacific sardine. Proceedings of the National Academy of Sciences 110:6430-6435.

Deyle, E. R., and G. Sugihara. 2011. Generalized Theorems for Nonlinear State Space Reconstruction. PLoS ONE 6:e18295.

Dixon, P. A., M. J. Milicich, and G. Sugihara. 1999. Episodic Fluctuations in Larval Supply. Science 283:1528-1530.

Fromentin, J.-M., and J. E. Powers. 2005. Atlantic bluefin tuna: population dynamics, ecology, fisheries and management. Fish and Fisheries 6:281-306.

Garcia, A., F. Alemany, P. Velez-Belchi, J. L. López Jurado, D. Cortés, J. M. de la Serna, C. González Pola, J. M. Rodríguez, J. Jansá, and T. Ramírez. 2005. Characterization of the bluefin tuna spawning habitat off the Balearic Archipelago in relation to key hydrographic features and associated environmental conditions. Col. Vol. Sci. Pap. ICCAT 58:535-549.

Glaser, S. M., M. J. Fogarty, H. Liu, I. Altman, C.-H. Hsieh, L. Kaufman, A. D. MacCall, A. A. Rosenberg, H. Ye, and G. Sugihara. 2013. Complex dynamics may limit prediction in marine fisheries. Fish and Fisheries: 1-18.

Glaser, S. M., H. Ye, M. Maunder, A. MacCall, M. Fogarty, and G. Sugihara. 2011. Detecting and forecasting complex nonlinear dynamics in spatially structured catch-per-unit-effort time series for North Pacific albacore (*Thunnus alalunga*). Canadian Journal of Fisheries and Aquatic Sciences 68:400-412.

Govoni, J. J. 2005. Fisheries oceanography and the ecology of early life histories of fishes: a perspective over fifty years. Sci. Mar. 69(Suppl. 1):125-137.

Hsieh, C., C. Anderson, and G. Sugihara. 2008. Extending Nonlinear Analysis to Short Ecological Time Series. The American Naturalist 171:71-80.

Hsieh, C., and M. D. Ohman. 2006. Biological responses to environmental forcing: the linear tracking window hypothesis. Ecology 87:1932-1938.

Hsieh, C., C. Reiss, W. Watson, M. J. Allen, J. R. Hunter, R. N. Lea, R. H. Rosenblatt, P. E. Smith, and G. Sugihara. 2005. A comparison of long-term trends and variability in populations of larvae of exploited and unexploited fishes in the Southern California region: A community approach. Progress in Oceanography 67:160-185.

Kimura, S., Y. Kato, T. Kitagawa, and N. Yamaoka. 2010. Impacts of environmental variability and global warming scenario on Pacific bluefin tuna (*Thunnus orientalis*) spawning grounds and recruitment habitat. Progress in Oceanography 86:39-44.

Kitagawa, T., Y. Kato, M. J. Miller, Y. Sasai, H. Sasaki, and S. Kimura. 2010. The restricted spawning area and season of Pacific bluefin tuna facilitate use of nursery areas: A modeling approach to larval and juvenile dispersal processes. Journal of Experimental Marine Biology and Ecology 393:23-31.

Kitagawa, T., S. Kimura, H. Nakata, and H. Yamada. 2006. Thermal adaptation of Pacific bluefin tuna *Thunnus orientalis* to temperate waters. Fisheries Science 72:149-156.

Kitagawa, T., H. Nakata, S. Kimura, T. Itoh, S. Tsuji, and A. Nitta. 2000. Effect of ambient temperature on the vertical distribution and movement of Pacific bluefin tuna *Thunnus thynnus orientalis*. Marine Ecology Progress Series 206:251-260.

Lindo-Atichati, D., F. Bringas, G. Goni, B. Muhling, F. Muller-Karger, and S. Habtes. 2012. Varying mesoscale structures influence larval fish distribution in the northern Gulf of Mexico. Marine Ecology Progress Series 463:245-257.

Liu, H., M. Fogarty, S. Glaser, I. Altman, C. Hsieh, L. Kaufman, A. Rosenberg, and G. Sugihara. 2012. Nonlinear dynamic features and co-predictability of the Georges Bank fish community. Marine Ecology Progress Series 464:195-207.

Liu, H., M. J. Fogarty, J. A. Hare, C. Hsieh, S. M. Glaser, H. Ye, E. Deyle, and G. Sugihara. 2014. Modeling dynamic interactions and coherence between marine zooplankton and fishes linked to environmental variability. Journal of Marine Systems 131:120-129.

Masuda, R., J. Shoji, M. Aoyama, and M. Tanaka. 2002. Chub mackerel larvae fed fish larvae can swim faster than those fed rotifers and Artemia nauplii. Fisheries Science 68:320-324.

Matsuura, H., T. Sugimoto, M. Nakai, and S. Tsuji. 1997. Oceanographic conditions near the spawning ground of southern bluefin tuna; northeastern Indian Ocean. Journal of Oceanography 53:421-434.

McGowan, M. F., and W. J. Richards. 1989. Bluefin tuna, *Thunnus thynnus*, larvae in the Gulf Stream off the Southeastern United States: satellite and shipboard observations of their environment. Fishery Bulletin 87:615-631.

Muhling, B. A., P. Reglero, L. Ciannelli, D. Alvarez-Berastegui, F. Alemany, J. Lamkin, and M. A. Roffer. 2013. Comparison between environmental characteristics of larval bluefin tuna *Thunnus thynnus* habitat in the Gulf of Mexico and western Mediterranean Sea. Marine Ecology Progress Series 486:257-276.

Myers, R. A. 1998. When Do Environment–recruitment Correlations Work? Reviews in Fish Biology and Fisheries 8:285-305.

Myers, R. A., G. Mertz, and C. A. Bishop. 1993. Cod spawning in relation to physical and biological cycles of the northern North–west Atlantic. Fisheries Oceanography 2:154-165.

National Climatic Data Center/NESDIS/NOAA/U.S. (n.d.). Department of Commerce, Data Support Section/Computational and Information Systems Laboratory/National Center for Atmospheric Research/University Corporation for Atmospheric Research, Earth System Research Laboratory/NOAA/U.S.

Department of Commerce, and Cooperative Institute for Research in Environmental Sciences/University of Colorado, 1984: International Comprehensive Ocean-Atmosphere Data Set (ICOADS) Release 2.5, Monthly Summaries. Research Data Archive at the National Center for Atmospheric Research, Computational and Information Systems Laboratory, Boulder, CO. [Available online at http://dx.doi.org/10.5065/D6CF9N3F.] Accessed 04 Aug 2014.

Perretti, C. T., S. B. Munch, and G. Sugihara. 2013. Model-free forecasting outperforms the correct mechanistic model for simulated and experimental data. Proceedings of the National Academy of Sciences 110:5253-5257.

Ravier, C., and J.-M. Fromentin. 2004. Are the long-term fluctuations in Atlantic bluefin tuna (*Thunnus thynnus*) population related to environmental changes? Fisheries Oceanography 13:145-160.

Reglero, P., A. Urtizberea, A. P. Torres, F. Alemany, and Fiksen. 2011. Cannibalism among size classes of larvae may be a substantial mortality component in tuna. Marine Ecology Progress Series 433:205-219.

Satoh, K. 2010. Horizontal and vertical distribution of larvae of Pacific bluefin tuna *Thunnus orientalis* in patches entrained in mesoscale eddies. Marine Ecology Progress Series 404:227-240.

Satoh, K., Y. Tanaka, and M. Iwahashi. 2008. Variations in the instantaneous mortality rate between larval patches of Pacific bluefin tuna *Thunnus orientalis* in the northwestern Pacific Ocean. Fisheries Research 89:248-256.

Steele, J. H., and E. W. Henderson. 1984. Modeling Long-Term Fluctuations in Fish Stocks. Science 224:985-987.

Sugihara. 1994. Nonlinear forecasting for the classification of natural time series. Philosophical Transactions of the Royal Society of London Series a-Mathematical Physical and Engineering Sciences 348:477-495.

Sugihara, G., W. Allan, D. Sobel, and K. D. Allan. 1996. Nonlinear control of heart rate variability in human infants. Proceedings of the National Academy of Sciences 93:2608-2613.

Sugihara, G., and R. M. May. 1990. Nonlinear forecasting as a way of distinguishing chaos from measurement error in time series. Nature 344:734-741.

Sugihara, G., R. May, H. Ye, C. -h. Hsieh, E. Deyle, M. Fogarty, and S. Munch. 2012. Detecting Causality in Complex Ecosystems. Science 338:496-500.

Takens, F. 1981. Detecting strange attractors in turbulence. Pages 366–381 in D. Rand and L.-S. Young, editors. Dynamical Systems and Turbulence, Warwick 1980. Springer Berlin Heidelberg.

Tanaka, Y., M. Mohri, and H. Yamada. 2007. Distribution, growth and hatch date of juvenile Pacific bluefin tuna Thunnus orientalis in the coastal area of the Sea of Japan. Fisheries Science 73:534-542.

Tanaka, Y., K. Satoh, M. Iwahashi, and H. Yamada. 2006. Growth-dependent recruitment of Pacific bluefin tuna *Thunnus orientalis* in the northwestern Pacific Ocean. Marine Ecology Progress Series 319:225–235.

Teo, S. L. H., and B. A. Block. 2010. Comparative Influence of Ocean Conditions on Yellowfin and Atlantic Bluefin Tuna Catch from Longlines in the Gulf of Mexico. PLoS ONE 5:e10756.

Teo, S. L. H., A. M. Boustany, and B. A. Block. 2007. Oceanographic preferences of Atlantic bluefin tuna, *Thunnus thynnus*, on their Gulf of Mexico breeding grounds. Marine Biology 152:1105–1119.

Ward, E. J., E. E. Holmes, J. T. Thorson, and B. Collen. 2014. Complexity is costly: a meta-analysis of parametric and non-parametric methods for short-term population forecasting. Oikos 123:652-661.

Table 1. The effects of spawning stock biomass (SSB) and monthly sea surface temperature (SST) on recruitment of eastern Atlantic bluefin tuna. Multivariate SSR models with significant improvement in forecast skill relative to univariate SSR are shown. ρ is Pearson correlation calculated in the original data units, $\Delta F_{\text{univariate}} = \rho_{\text{multivariate}} - \rho_{\text{univariate}}$, and $\Delta F_{\text{naive}} = \rho_{\text{multivariate}} - \rho_{\text{naive}}$, where naïve method refers to the use of observed recruitment at *t* as a predictor of recruitment at *t+1*.

Model type	ρ	$\Delta F_{\text{univariate}}$	ΔF_{naive}
SSB	0.804	0.134	0.077
Large bounding box			
February SST	0.739	0.027	0.005
April SST	0.710	0.073	-0.017
June SST	0.744	0.019	0.015
July SST	0.757	0.043	0.023
August SST	0.757	0.043	0.023
September SST	0.757	0.079	0.039
October SST	0.730	0.013	-0.004
November SST	0.739	0.027	0.005
Small bounding box			
September SST	0.732	0.033	0.005
October SST	0.724	0.017	-0.010

Table 2. The effects of spawning stock biomass (SSB) and monthly sea surface temperature (SST) on recruitment of western Atlantic bluefin tuna. Multivariate SSR models with significant improvement in forecast skill relative to univariate SSR are shown. ρ is Pearson correlation calculated in the original data units, $\Delta F_{\text{univariate}} = \rho_{\text{multivariate}} - \rho_{\text{univariate}}$, and $\Delta F_{\text{naive}} = \rho_{\text{multivariate}} - \rho_{\text{naive}}$, where Naïve method refers to the use of observed recruitment at *t* as a predictor of recruitment at *t+1*.

Model type	ρ	$\Delta F_{\text{univariate}}$	ΔF_{naive}
SSB	0.461	0.007	-0.090
West of Loop Current			
April SST	0.377	0.067	0.074
North of Loop Current			
May SST	0.423	0.181	-0.009

Table 3. The effects of monthly sea surface temperature (SST) on recruitment of North Pacific bluefin tuna. Multivariate SSR models with significant improvement in forecast skill relative to univariate SSR are shown. ρ is Pearson correlation calculated in the original data units, $\Delta F_{\text{univariate}} = \rho_{\text{multivariate}} - \rho_{\text{univariate}}$, and $\Delta F_{\text{naive}} = \rho_{\text{multivariate}} - \rho_{\text{naive}}$, where Naïve method refers to the use of observed recruitment at *t* as a predictor of recruitment at *t+1*.

Model type	ρ	$\Delta F_{\text{univariate}}$	ΔF_{naive}
SSB	0.281	0.257	0.272
Sea of Japan			
August SST	0.321	0.276	0.312
December SST	0.157	0.119	0.148
January SST +1 year	0.287	0.268	0.278
Ryukyu Islands large box			
August SST	0.366	0.358	0.357
November SST	0.111	0.135	0.192
Ryukyu Islands small box			
August SST	0.448	0.424	0.439
September SST	0.306	0.276	0.297
South of Japan			
July SST	0.300	0.254	0.291
September SST	0.259	0.246	0.250
November	0.193	0.263	0.224

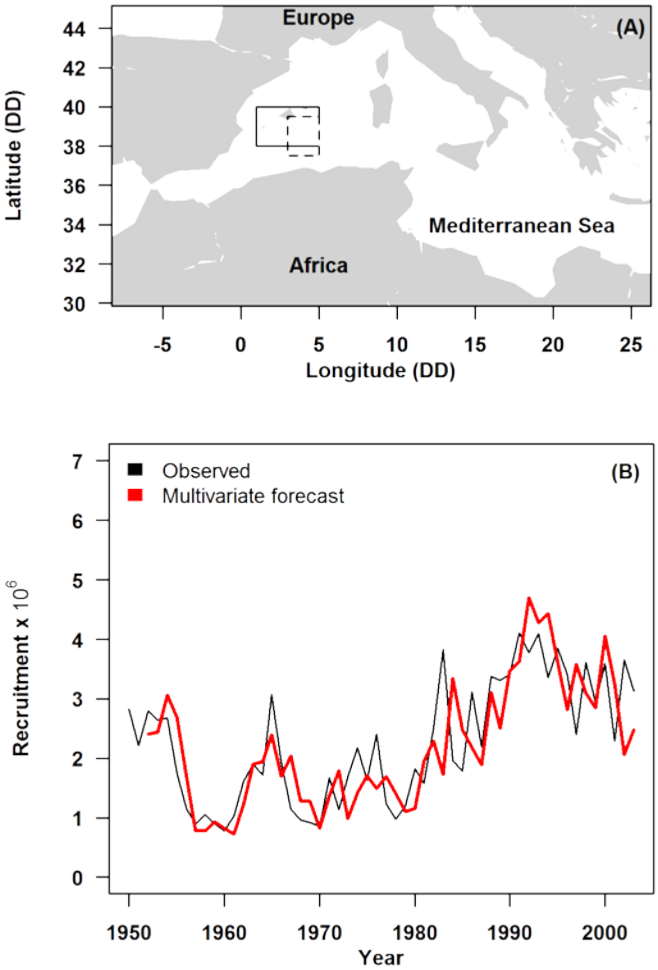

Figure 1. (A) Mediterranean Sea with large (solid line) and small (dashed line) rectangular boundaries used to summarize sea surface temperature. (B) Recruitment in numbers and forecasts from multivariate state-space reconstruction based on inclusion of both spawning stock biomass and September sea surface temperature in the larger bounding box.

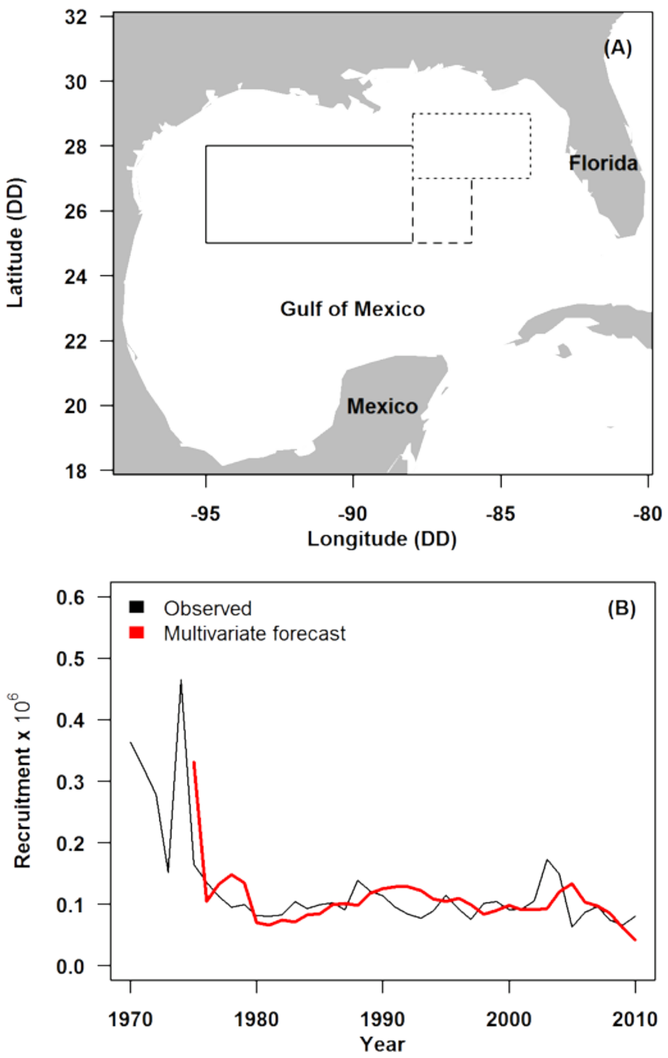

Figure 2. (A) Gulf of Mexico with bounding boxes used to summarize sea surface temperature according to the Loop Current region of influence (dashed line), area west of the Loop Current (solid line) and area north of the Loop Current (dotted line). (B) Recruitment in numbers and forecasts from multivariate state-space reconstruction based on inclusion of both spawning stock biomass and April sea surface temperature west of the Loop Current.

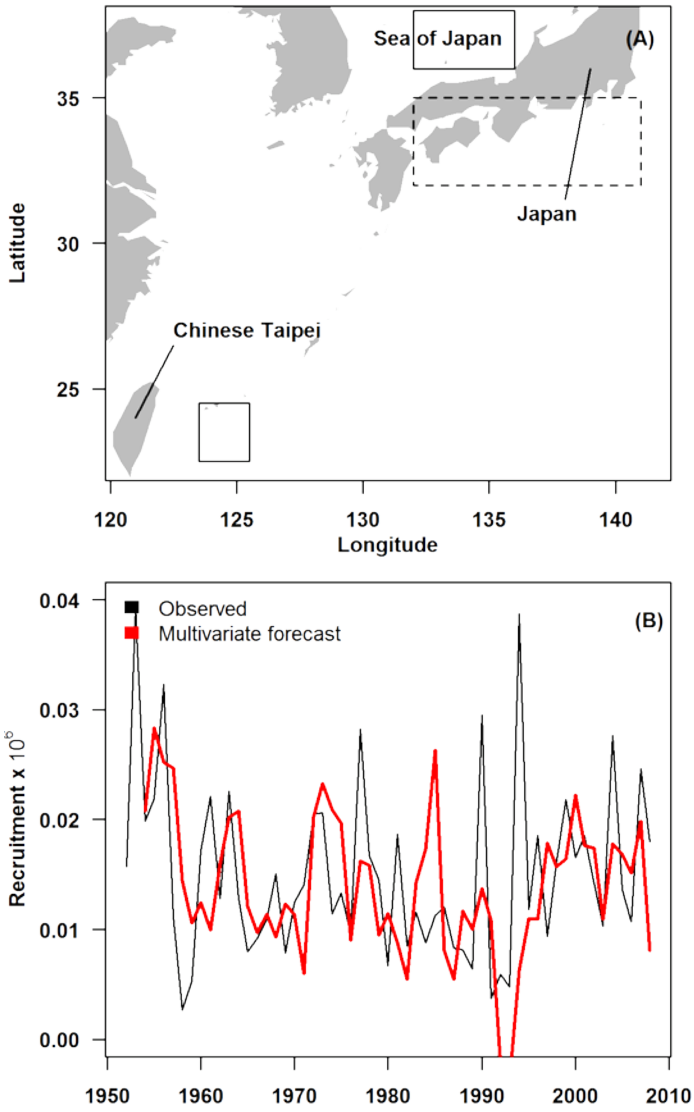

Figure 3. (A) North Pacific with bounding boxes used to summarize sea surface temperature according areas associated with spawning distribution (solid lines) and areas associated with nursery grounds (dashed lines. (B) Recruitment in numbers and forecast based on August sea surface temperature near Ryukyu Islands & Sea of Japan.

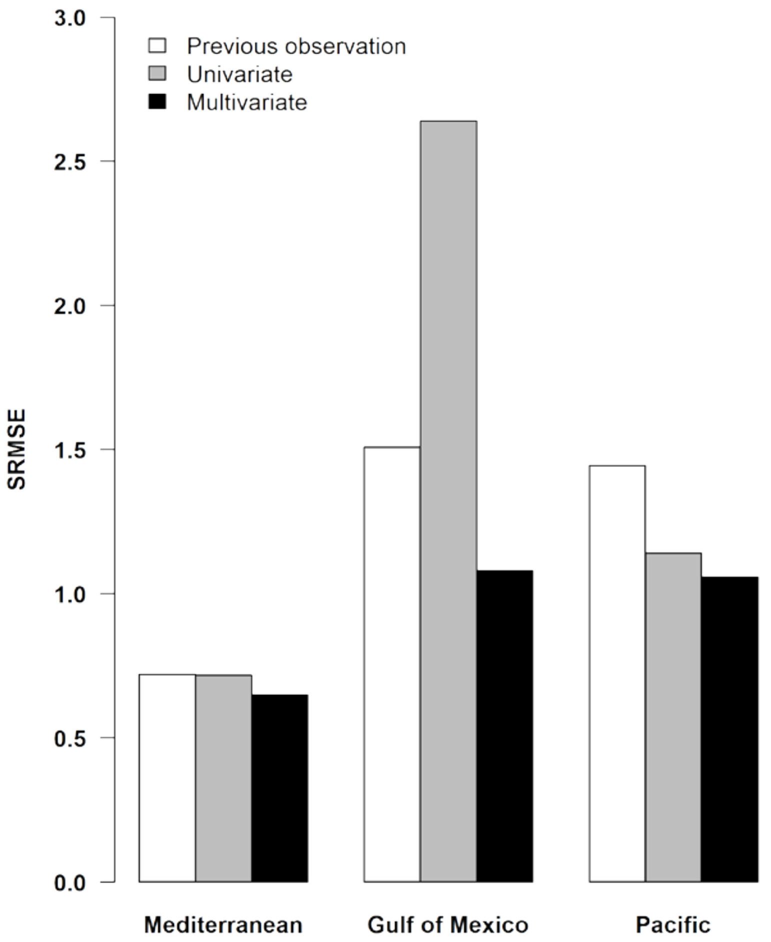

Figure 4. Performance of multivariate state-space reconstruction (SSR) models illustrated in **Figures 1b, 2b, & 3b**. Out-of-sample forecast skill is reported as standardized root mean square error (SRMSE).